Research Article
Experimental and Translational Hepatology

JOURNAL
OF HEPATOLOGY

TGF-β1-driven reduction of cytoglobin leads to oxidative DNA damage in stellate cells during non-alcoholic steatohepatitis

Graphical abstract

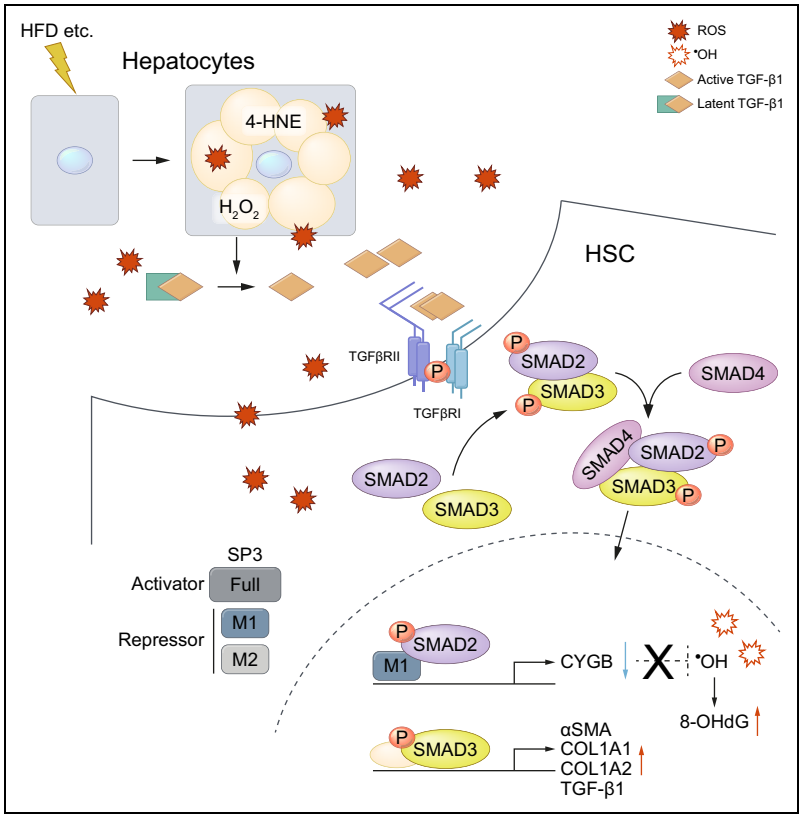

Highlights

- Reactive oxygen species levels are increased in advanced NASH-related fibrosis.
- *CYGB* directly scavenges ·OH and attenuates 8-OHdG generation in human HSCs.
- *CYGB* downregulation by TGF-β1 leads to oxidative DNA damage in human HSCs.
- TGF-β1 suppresses *CYGB* expression in human HSCs via the pSMAD2/SP3-M1 pathway.
- *CYGB* expression is absent in $pSMAD2^{+}8\text{-}OHdG^{+}$ HSCs in NASH-related fibrosis.

Authors

Yoshinori Okina, Misako Sato-Matsubara, Tsutomu Matsubara, …, Katsutoshi Yoshizato, Massimo Pinzani, Norifumi Kawada

Correspondence

kawadanori@med.osaka-cu.ac.jp
(N. Kawada).

Lay summary

Cytoglobin (*CYGB*) is a respiratory protein that acts as a scavenger of reactive oxygen species and protects cells from oxidative DNA damage. Herein, we show that the cytokine TGF-β1 downregulates human *CYGB* expression. This leads to oxidative DNA damage in activated hepatic stellate cells. Our findings provide new insights into the relationship between *CYGB* expression and the pathophysiology of fibrosis in patients with non-alcoholic steatohepatitis.

https://doi.org/10.1016/j.jhep.2020.03.051

 J. Hepatol. 2020, 73, 882–895

Research Article
Experimental and Translational Hepatology

JOURNAL OF HEPATOLOGY

TGF-β1-driven reduction of cytoglobin leads to oxidative DNA damage in stellate cells during non-alcoholic steatohepatitis

Yoshinori Okina[1,‡], Misako Sato-Matsubara[1,2,‡], Tsutomu Matsubara[3], Atsuko Daikoku[1], Lisa Longato[4], Krista Rombouts[4], Le Thi Thanh Thuy[1], Hiroshi Ichikawa[5], Yukiko Minamiyama[6], Mitsutaka Kadota[7], Hideki Fujii[1], Masaru Enomoto[1], Kazuo Ikeda[3], Katsutoshi Yoshizato[2], Massimo Pinzani[4], Norifumi Kawada[1,*]

[1]Departments of Hepatology, [2]Endowed Laboratory of Synthetic Biology, [3]Anatomy and Regenerative Biology, Graduate School of Medicine, Osaka City University, Osaka 545-8585, Japan; [4]Regenerative Medicine and Fibrosis Group, Institute for Liver and Digestive Health, University College London, Royal Free Hospital, London, NW3 2PF, United Kingdom; [5]Department of Medical Life Systems, Faculty of Life and Medical Sciences, Doshisha University, Kyoto 610-0321, Japan; [6]Food Hygiene and Environmental Health, Division of Applied Life Science, Graduate School of Life and Environmental Sciences, Kyoto Prefectural University, Kyoto 606-8522, Japan; [7]Laboratory for Phyloinformatics, RIKEN Center for Biosystems Dynamics Research, Hyogo 650-0047, Japan

Background & Aims: Cytoglobin (*CYGB*) is a respiratory protein that acts as a scavenger of reactive oxygen species. The molecular role of *CYGB* in human hepatic stellate cell (HSC) activation and human liver disease remains uncharacterised. The aim of this study was to reveal the mechanism by which the TGF-β1/SMAD2 pathway regulates the human *CYGB* promoter and the pathophysiological function of *CYGB* in human non-alcoholic steatohepatitis (NASH).

Methods: Immunohistochemical staining was performed using human NASH biopsy specimens. Molecular and biochemical analyses were performed by western blotting, quantitative PCR, and luciferase and immunoprecipitation assays. Hydroxyl radicals (•OH) and oxidative DNA damage were measured using an •OH-detectable probe and 8-hydroxy-2′-deoxyguanosine (8-OHdG) ELISA.

Results: In culture, TGF-β1-pretreated human HSCs exhibited lower *CYGB* levels – together with increased NADPH oxidase 4 (NOX4) expression – and were primed for H_2O_2-triggered •OH production and 8-OHdG generation; overexpression of human *CYGB* in human HSCs reversed these effects. Electron spin resonance demonstrated the direct •OH scavenging activity of recombinant human CYGB. Mechanistically, pSMAD2 reduced *CYGB* transcription by recruiting the M1 repressor isoform of SP3 to the human *CYGB* promoter at nucleotide positions $^{+}2$–$^{+}13$ from the transcription start site. The same repression did not occur on the mouse *Cygb* promoter. TGF-β1/SMAD3 mediated αSMA and collagen expression. Consistent with observations in cultured human HSCs, *CYGB* expression was negligible, but 8-OHdG was abundant, in activated αSMA^{+}pSMAD2^{+}- and αSMA^{+}NOX4^{+}-positive hepatic stellate cells from patients with NASH and advanced fibrosis.

Conclusions: Downregulation of *CYGB* by the TGF-β1/pSMAD2/SP3-M1 pathway brings about •OH-dependent oxidative DNA damage in activated hepatic stellate cells from patients with NASH.

Lay summary: Cytoglobin (*CYGB*) is a respiratory protein that acts as a scavenger of reactive oxygen species and protects cells from oxidative DNA damage. Herein, we show that the cytokine TGF-β1 downregulates human *CYGB* expression. This leads to oxidative DNA damage in activated hepatic stellate cells. Our findings provide new insights into the relationship between *CYGB* expression and the pathophysiology of fibrosis in patients with non-alcoholic steatohepatitis.

Introduction

Hepatic fibrosis is a common feature of many chronic liver diseases. Hepatic fibrosis ultimately progresses to cirrhosis and increases the risk of hepatocellular carcinoma (HCC).[1] Severe hepatic fibrosis and HCC are estimated to cause 3.5% of all deaths worldwide,[2] indicating a need for new anti-fibrotic therapies based on a detailed mechanistic understanding of liver disease.[3] The activation of hepatic stellate cells (HSCs) into contractile and matrix-producing myofibroblasts (MFBs) is a central event in liver fibrosis. HSC activation is triggered by multiple mediators secreted by damaged hepatocytes, activated macrophages, and aggregated platelets. Among the HSC-activating factors, transforming growth factor β1 (TGF-β1) is a key molecule that regulates MFB function.[4] In chronic liver disease, MFBs persist, become highly proliferative and migratory, and continuously deposit extracellular matrix (ECM) to replace hepatic parenchyma.

Cytoglobin (CYGB) is a mammalian globin expressed in HSCs that binds oxygen, carbon monoxide, and nitric oxide[5,6] and protects organs and cells against oxidative stress.[7,8] Recombinant rat *Cygb* was reported to increase the expression of antioxidant

Keywords: NAFLD/NASH; Liver fibrosis; Cytoglobin; TGF-β1; Oxidative stress; Hepatic stellate cells.
Received 27 August 2019; received in revised form 28 March 2020; accepted 31 March 2020; available online 21 April 2020

* Corresponding author. Address: Department of Hepatology, Graduate School of Medicine, Osaka City University, 1-4-3, Asahimachi, Abeno, Osaka 545-8585. Tel.: +81-6-6645-3897.
E-mail address: kawadanori@med.osaka-cu.ac.jp (N. Kawada).
‡ These authors contributed equally to this work.

https://doi.org/10.1016/j.jhep.2020.03.051

Table 1. Clinical and biochemical characteristics of the patients with biopsy-proven NAFLD/NASH.

Characteristics	All (n = 13)	No advanced fibrosis (stage 0–2) (n = 8)	Advanced fibrosis (stage 3–4) (n = 5)	*p* value
Demographics				
Age (years)	55.9 ± 15.1	51.1 ± 17.7	63.6 ± 3.7	0.377
Gender				
Female	8 (61.5)	3 (37.5)	5 (100.0)	0.075
Male	5 (38.5)	5 (62.5)	0 (0.0)	
BMI (kg/m^2)	26.3 ± 3.3	26.5 ± 3.5	26.1 ± 3.4	0.770
Biological data				
AST (U/L)	50.2 ± 29.9	47.5 ± 33.8	54.6 ± 25.2	0.341
ALT (U/L)	63.8 ± 52.4	70.5 ± 61.5	53.2 ± 37.3	0.942
GGT (U/L)	75.1 ± 42.8	84.4 ± 49.6	60.2 ± 27.0	0.341
Total bilirubin (mg/dl)	0.86 ± 0.24	0.80 ± 0.26	0.96 ± 0.19	0.262
Direct bilirubin (mg/dl)	0.29 ± 0.08	0.29 ± 0.08	0.3 ± 0.07	0.753
Albumin (g/dl)	4.1 ± 0.38	4.3 ± 0.27	3.8 ± 0.34	0.022
Triglycerides (mg/dl)	99.2 ± 35.3	104.6 ± 37.6	90.4 ± 33.2	0.770
Total cholesterol (mg/dl)	187.6 ± 40.9	184.8 ± 36.0	192.2 ± 51.9	0.999
Platelet count (10^9/L)	207.8 ± 68.9	239.4 ± 49.7	157.2 ± 68.7	0.040
Glucose (mg/dl)	120.8 ± 34.9	131.9 ± 40.0	103.0 ± 14.1	0.164
Clincal prediction rules				
NAFLD fibrosis score	0.09 ± 0.93	0.07 ± 0.62	0.11 ± 1.38	0.884
FIB-4 index	2.15 ± 1.42	1.34 ± 0.89	3.43 ± 1.14	0.008
Histology				
NAS, n (%)				
Steatosis				
0	1 (7.7)	1 (12.5)	0 (0.0)	
1	6 (46.2)	3 (37.5)	3 (60.0)	
2	3 (23.1)	1 (12.5)	2 (40.0)	
3	3 (23.1)	3 (37.5)	0 (0.0)	
Ballooning				
0	6 (46.2)	6 (75.0)	0 (0.0)	
1	2 (15.4)	0 (0.0)	2 (40.0)	
2	5 (38.5)	2 (25.0)	3 (60.0)	
Inflammation				
0	3 (23.1)	3 (37.5)	0 (0.0)	
1	5 (38.5)	4 (50.0)	1 (20.0)	
2	3 (23.1)	0 (0.0)	3 (60.0)	
3	2 (15.4)	1 (12.5)	1 (20.0)	
Fibrosis, n (%)				
0	2 (15.4)	2 (25.0)	0 (0.0)	
1	4 (30.8)	4 (50.0)	0 (0.0)	
2	2 (15.4)	2 (25.0)	0 (0.0)	
3	3 (23.1)	0 (0.0)	3 (60.0)	
4	2 (15.4)	0 (0.0)	2 (40.0)	

P values were obtained using *t* test for continuous variables.
ALT, alanine aminotransferase; AST, aspartate aminotransferase; BMI, body mass index; FIB-4, fibrosis-4; GGT, gamma-glutamyltransferase; NAFLD, non-alcoholic fatty liver disease; NAS, NAFLD Activity Score; NASH, non-alcoholic steatohepatitis.

enzymes and to inhibit collagen (COL) III and IV expression in CCl_4-induced liver fibrosis.[9] We previously demonstrated that *Cygb*$^{-/-}$ mice are susceptible to diethylnitrosamine-induced development of liver cancer[10] and exhibit augmented hepatic inflammation, fibrosis, and tumour occurrence when fed a high-fat diet or subjected to bile-duct ligation.[11,12] Conversely, thioacetamide-induced liver fibrosis was attenuated in HSC-specific *Cygb* transgenic mice.[13]

The regulation of *CYGB* transcription and the role of *CYGB* in human fibrotic liver disease remain largely uncharacterised. *Cygb* expression was upregulated in mice exposed to hypoxia, whereas *Cygb* induction was lost in hypoxia-inducible factor 1α-knockout mice.[14] Furthermore, hypoxia response elements were identified in the *Cygb* promoter region.[15] Those results suggest that the regulation of *Cygb* expression is oxygen dependent. By contrast, we recently reported that fibroblast growth factor 2 (FGF2) induces *CYGB* via c-JUN N-terminal kinase (JNK)-c-JUN signals in human HSCs.[16]

Herein, we show that TGF-β1 supresses human *CYGB* expression through phosphorylated SMAD2 (pSMAD2) and the M1 repressor isoform of SP3. The TGF-β1-induced suppression of *CYGB* causes a loss of cellular tolerance to exogenous oxidative stress and oxidative DNA damage in human HSCs. Our results provide a new insight into the pathophysiology of NASH-related fibrosis.

Materials and methods

Human tissue specimens

Patients with biopsy-proven non-alcoholic fatty liver disease (NAFLD)/non-alcoholic steatohepatitis (NASH) were recruited at Osaka City University Hospital (Osaka, Japan; Table 1). Thirteen liver biopsy specimens were obtained using a 16-gauge

MAX-Core needle (Bard Biopsy Systems, AZ, USA). The samples were fixed in 10% formalin and stained with H&E. Each specimen was evaluated by experienced pathologists that were blinded to the clinical findings.

ELISA for 8-OHdG

DNA was purified using a DNA Extract WB kit (Wako Pure Chemical Industries Ltd.) and subjected to ELISA for 8-OHdG according to the manufacturer's protocol. Intracellular 8-OHdG concentrations were measured by absorbance at 450 nm. The 8-OHdG standards used for the assay ranged between 0 ng/ml and 10 ng/ml.

Immunoprecipitation analysis

Cells were harvested with ice-cold PBS and lysed in TNE Buffer (50 mM Tris-HCl [pH 7.4], 0.1% NP-40, 100 mM NaCl, and 1 mM EDTA) containing protease inhibitors (Roche Diagnostics, Mannheim, Germany) and phosphatase inhibitors (Thermo Fisher Scientific, Waltham, MA, USA). The cell extracts (2 mg/450 μl) were pre-cleaned with protein G magnetic beads (20 μl of a 50% bead slurry, Thermo Fisher Scientific) at 4°C for 60 min. The samples were then incubated with anti-SMAD2 antibody or normal rabbit IgG at 4°C overnight and subjected to SDS-PAGE by western blot analysis.

Statistics and reproducibility

All experiments were replicated at least 3 times. Differences among experimental groups were analysed using unpaired *t* test, Mann-Whitney *U* test, or one-way or two-way ANOVA performed using the GraphPad Prism 6 software (La Jolla, CA, USA). *P* values less than 0.05 were considered statistically significant. The data are displayed as the mean ± SD. Significant differences among groups are indicated as $^{*}p$ <0.05, $^{**}p$ <0.01, and $^{***}p$ <0.001.

For further details regarding the materials and methods used, please refer to the CTAT table and supplementary information.

Results

Involvement of *CYGB* in reactive oxygen species (ROS) production and HSC activation in human liver fibrosis

Oxidative stress has been implicated in the pathogenesis of NAFLD/NASH with lobular inflammation and fibrosis.[17] We measured the expression of 4-hydroxy-2′-nonenal (4-HNE), an end product of lipid peroxidation, and 8-hydroxy-2′-deoxyguanosine (8-OHdG), a marker of oxidative DNA damage, in liver tissues from patients with biopsy-proven NAFLD/NASH with stage F0–F4 fibrosis (Table 1). As previously described,[18] 4-HNE-positive staining was limited in patients with stage F0 fibrosis but was more pronounced in patients with more advanced fibrosis, especially those with stage F4 fibrosis (p <0.05; Fig. 1A). A previous study reported that 4-HNE accumulated in destroyed hepatocytes and was discharged from those cells into the space of Disse,[19] representing a source of oxidative stress in hepatic sinusoids. We did not observe any 8-OHdG-positive signal in cells from patients with stage F0 fibrosis, but 8-OHdG-staining was dominant in hepatocytes from patients with stage F1 fibrosis and abundant in both hepatocytes and stromal cells from patients with stage F4 fibrosis (Fig. 1B and Fig. S1A). Double-immunohistochemical (IHC) staining revealed co-localisation of 8-OHdG and α-smooth muscle actin (αSMA) in the stroma of patients with stage F4 disease (Fig. 1C).

Based on our observations of human NAFLD/NASH biopsy specimens, we hypothesised that activated HSCs become susceptible to oxidative stress. To confirm our hypothesis, we investigated the production of 2′,7′-dichlorofluorescin diacetate (DCFDA)-detectable ROS in cultured human HSCs (HHSteCs; ScienCell Research laboratories, San Diego, USA) and LX-2 (ATCC, Manassas, USA), which were pretreated with recombinant human (rh)TGF-β1 and then stimulated with hydrogen peroxide (H_2O_2). Treatment with 2 ng/ml rhTGF-β1 for 48 h resulted in slight increases in DCFDA-detectable ROS in the HHSteCs (p <0.05). The combination of rhTGF-β1 pre-treatment and subsequent H_2O_2 (0–640 μM) treatment augmented the ROS production in a dose-dependent manner (Fig. 1D). Similar results were obtained in HHSteCs challenged with H_2O_2 in the presence of rhTGF-β1, while LX-2, which lack *CYGB* expression, remained unresponsive to rhTGF-β1 in H_2O_2-dependent ROS production (Fig. S2A and B). In addition, ROS production by these HSCs was reconfirmed by dihydroethidium (DHE) assay except for DCFDA assay (Fig. S2C). To elucidate the reason why TGF-β1 treatment enhanced ROS production in the HHSteCs, we analysed the expression of several genes associated with antioxidative cellular defence: *CYGB*, *SOD1*, *GSR*, *CAT*, *GPX1*, *GSS*, *PRDX1* and *2, TXN* and *TXNRD1* in human HSCs. Of those genes, *CYGB* was the most strongly and dose-dependently downregulated by pre-treatment with rhTGF-β1 in HHSteCs (p <0.00001; Fig. 1E and Fig. S3A). Likewise, these antioxidant genes were regulated by TGF-β1 in LX-2, in which *CYGB* expression was lacking (Fig. S3B). Furthermore, the overexpression of *CYGB* in HHSteCs and LX-2 transfected with pCMV6 vector containing human *CYGB* reduced the enhancement of DCFDA-detectable ROS production in response to 2 ng/ml rhTGF-β1 followed by 320 μM H_2O_2, returning the ROS levels to those observed after treatment with 320 μM H_2O_2 alone (Fig. 1F and Fig. S3C–D). Western blots of lysates of cells that were subjected to the same experimental conditions revealed that αSMA and COL1A were induced after the treatment with rhTGF-β1 and/or H_2O_2, and that *CYGB* overexpression markedly reversed the induction at both protein and mRNA levels (Fig. 1G and Fig. S4A). We also confirmed that TGF-β1 significantly increased NADPH oxidase 4 (NOX4) and its expression was strongly reduced by the overexpression of *CYGB* (Fig. S4A). These results indicated that *CYGB* is involved in the attenuation of HSC activation as well as the suppression of ROS production in human HSCs.

CYGB scavenges hydroxyl radical (•OH) and protects TGF-β1-activated HSCs from DNA damage

Because we observed accumulation of 8-OHdG in αSMA-positive stromal cells from patients with NASH and advanced fibrosis, we hypothesised that the suppression of *CYGB* expression by rhTGF-β1 would result in the accumulation of oxidative DNA damage in HSCs due to •OH, which is the causative agent of 8-OHdG formation.[20] To test that, we monitored mitochondrial ROS production using the mitochondria-specific probe MitoTracker® Red CM-H_2XRos. After pre-treatment for 48 h with 2 ng/ml rhTGF-β1, HHSteCs were treated with 1 mM H_2O_2 for 1 h or with 100 μM antimycin A or 100 μM pyocyanin for 24 h to chemically induce •OH production. All 3 treatments induced MitoTracker® Red CM-H_2XRos-positive staining in HHSteCs pretreated with rhTGF-β1 (Fig. 2A and Fig. S5A).

Next, we focused on mitochondrial •OH production using *in vivo* imaging analysis with OxiORANGE™, a positively charged

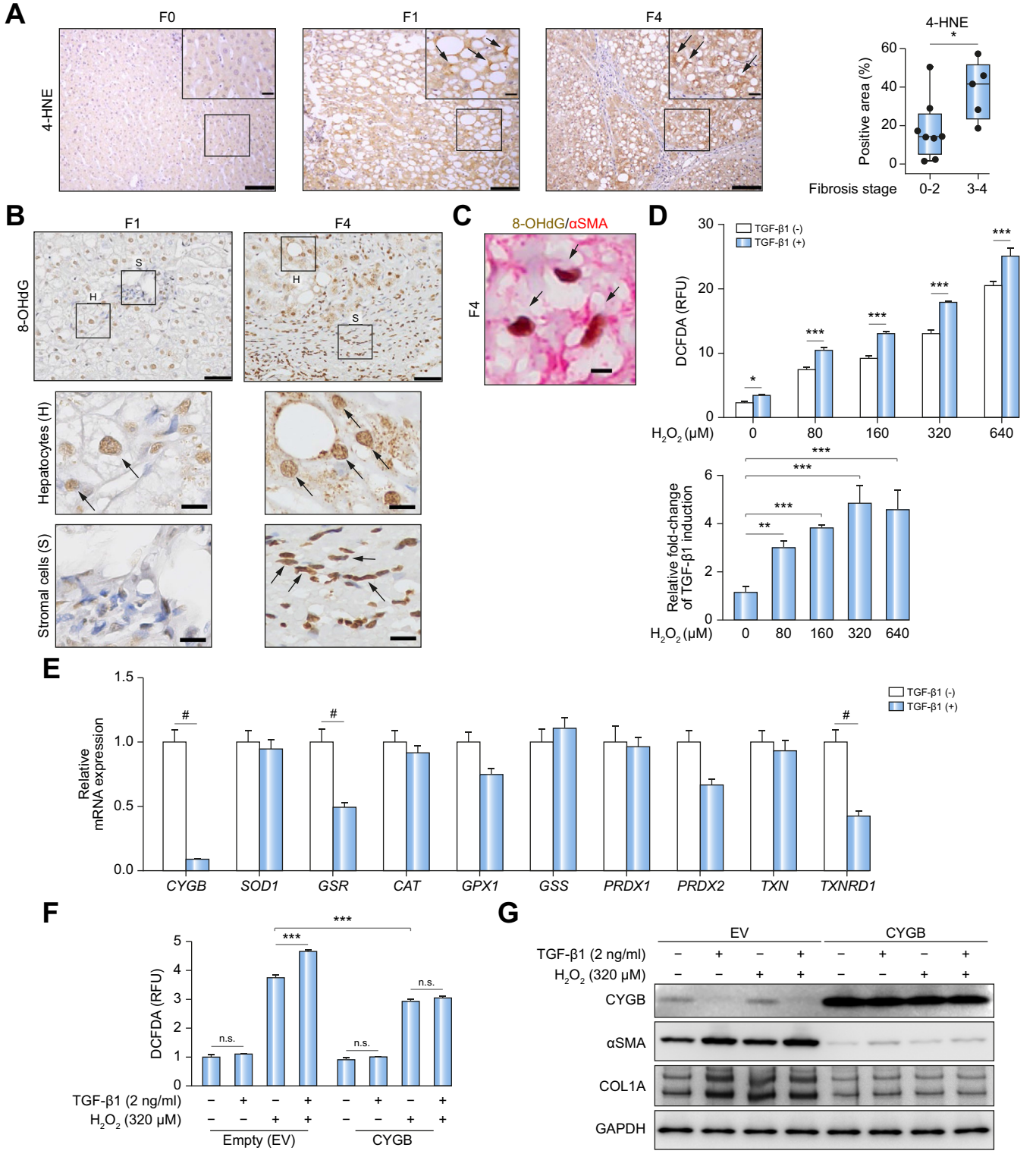

Fig. 1. Relationship between *CYGB* repression and intracellular ROS accumulation in activated HSCs and human liver tissues. (A and B) NAFLD/NASH specimens stained with (A) 4-HNE and (B) 8-OHdG (brown). Positive areas in (A) compared by *t* test, n = 13 (F0 n = 2, F1 n = 4, F4 n = 2). (C) Double-positive (8-OHdG/αSMA) stage-F4 stromal cells. Bars, 5 μm. (D) Intracellular ROS production. Relative fold change of DCFDA-detectable ROS production in response to 2 ng/ml rhTGF-β1 followed by H_2O_2 (0–640 μM) treatment compared with that in untreated controls. (E) Relative mRNA expression. #difference by multiple *t* tests with FDR of 1%. (F) Intracellular ROS production in cells transfected with pCMV6-EV or pCMV6-(*CYGB*). (G) Protein expression in transfected cells. Data expressed as means ± SD, n = 3. n.s.: not significant; **p* <0.05, ***p* <0.01, and ****p* <0.001 by ANOVA. Bars, 25 μm or 100 μm (enlarged views). DCFDA, 2′,7′-dichlorofluorescin diacetate; EV, empty vector; FDR, false discovery rate; H_2O_2, hydrogen peroxide; HSCs, hepatic stellate cells; 4-HNE, 4-hydroxy-2′-nonenal; NAFLD, non-alcoholic fatty liver disease; NASH, non-alcoholic steatohepatitis; 8-OHdG, 8-hydroxy-2′-deoxyguanosine; RFU, relative fluorescence unit; rh, recombinant human; ROS, reactive oxygen species.

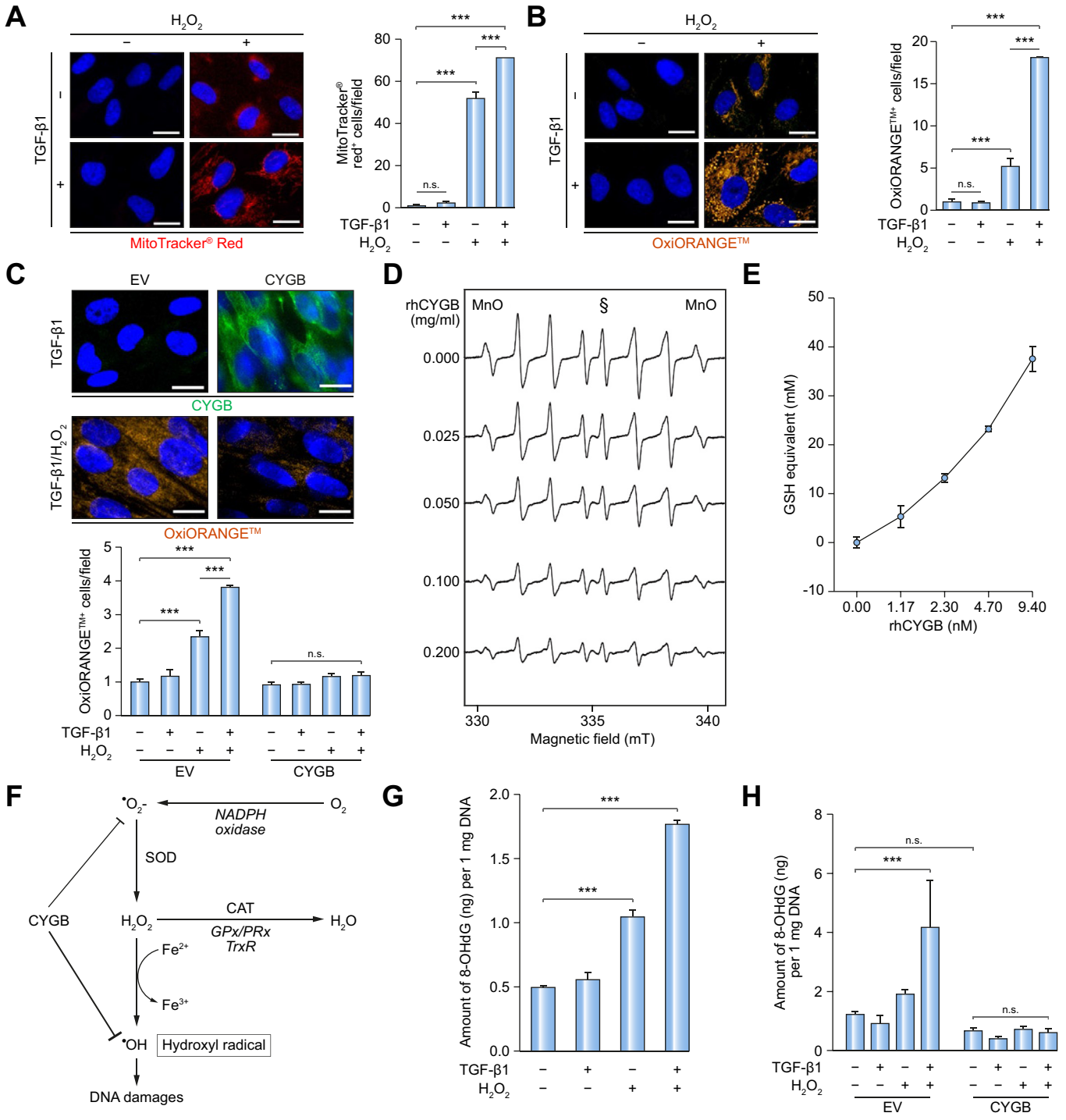

Fig. 2. The role of *CYGB* in •OH accumulation and cellular DNA damage induced by TGF-β1 and H_2O_2 in human HSCs. (A and B) H_2O_2-induced mitochondrial ROS (red, A) and intracellular •OH (orange, B) after TGF-β1 treatment. (C) Effect of *CYGB* overexpression on intracellular •OH generation. Immunofluorescence for human *CYGB* (green, upper) and OxiORANGE™ (orange, lower). (D) Scavenging of •OH by rhCYGB determined by ESR. MnO: manganese (II) oxide; mT: milliTesla; §: peak amplitude. (E) Concentration of rhCYGB converted to glutathione equivalent. (F) Formation of •OH and action of antioxidative genes. (G) Intracellular 8-OHdG formation in HHSteCs. (H) Effect of *CYGB* overexpression on 8-OHdG formation (ng) per 1 mg DNA. Data expressed as means ± SD, n = 3. n.s.: not significant; ***p <0.001 by ANOVA. Bars, 20 μm. ESR, electron spin resonance; EV, empty vector; H_2O_2, hydrogen peroxide; HHSteCs, human hepatic stellate cells; •OH, hydroxyl radical; 8-OHdG, 8-hydroxy-2′-deoxyguanosine; rh, recombinant human; ROS, reactive oxygen species.

orange fluorescent probe that detects •OH. We confirmed that pre-treatment with rhTGF-β1 augmented cellular •OH accumulation in response to H_2O_2, antimycin A, or pyocyanin treatment (Fig. 2B and Fig. S5B). Conversely, overexpression of *CYGB* markedly suppressed the rhTGF-β1/H_2O_2-induced accumulation of •OH in HHSteCs (Fig. 2C). To evaluate the •OH scavenging

properties of *CYGB*, we performed electron spin resonance (ESR) spectroscopy using the CYPMPO spin trap. We observed dose-dependent decreases in the amplitude of the ESR signal with the addition of rhCYGB (0.025–0.2 mg/ml) (Fig. 2D). We converted the •OH scavenging activity of 1 nmol rhCYGB to a 4.05 μmol glutathione equivalent (Fig. 2E). The results revealed that mitochondrial •OH levels were synergistically elevated by co-treatment with rhTGF-β1 and H_2O_2 and that •OH was scavenged by *CYGB* in HHSteCs (Fig. 2F).

Next, we used 8-OHdG ELISA to measure cellular oxidative DNA damage in HHSteCs after pre-treatment with 2 ng/ml rhTGF-β1 for 48 h and subsequent exposure to 320 μM H_2O_2 for 1 h. Treatment with rhTGF-β1 alone did not affect 8-OHdG generation (0.56 ± 0.06 ng per 1 mg DNA). Treatment with H_2O_2 alone induced a comparatively small increase in 8-OHdG (1.04 ± 0.06 ng per 1 mg DNA). However, rhTGF-β1 pre-treatment followed by H_2O_2 treatment induced cellular DNA damage at levels that were 3.6 times higher than those in untreated controls (1.77 ng ± 0.03 per 1 mg DNA; Fig. 2G). The overexpression of *CYGB* reduced the DNA damage levels, even after the combined treatment with rhTGF-β1 and H_2O_2 (Fig. 2H). Thus, TGF-β1 treatment followed by H_2O_2 treatment, but not H_2O_2 treatment alone, triggered a reduction in *CYGB*, resulting in impaired scavenging defences against •OH and increased oxidative DNA damage in HHSteCs.

TGF-β1 attenuates *CYGB* expression via SMAD2 and stimulates αSMA and type I collagen expression via SMAD3

Next, we investigated the molecular regulatory mechanism of the TGF-β1-induced downregulation of *CYGB* in HHSteCs. We used FGF2 as a *CYGB* inducer.[16] Treatment with 4 ng/ml FGF2 for 72 h increased *CYGB* expression and decreased αSMA expression at the protein and mRNA levels. By contrast, treatment with 2 ng/ml rhTGF-β1 for 72 h downregulated *CYGB* expression and upregulated αSMA expression compared with that in untreated controls (Fig. 3A and Fig. S6A). Other fibrosis-related growth factors (rhCTGF, PDGF-BB, and HGF) had negligible effects on *CYGB* protein expression (Fig. S6B). Treatment with rhTGF-β1 reduced *CYGB* and increased αSMA at both the protein level and the mRNA level in a dose-dependent (0–10 ng/ml) and time-dependent (0–48 h) manner (Fig. S6C and D).

In HHSteCs, rhTGF-β1 (2 ng/ml) phosphorylated canonical SMAD2 and SMAD3, starting at 15 min and reaching a peak at 1 h. In addition, ERK was present at 1 h and 4 h, but it failed to activate the AKT and JNK pathways (Fig. 3B and Fig. S6E–F). The TGF-β1-dependent phosphorylation of SMAD2 and SMAD3 was completely blocked by 1 μM SB431542 (Fig. S7A). SB431542 also blocked the repression of *CYGB* expression as well as the induction of TGF-β1-target genes such as αSMA, TGF-β1, and COL1A1 in untreated and rhTGF-β1-treated HHSteCs (Fig. 3C and D). To determine the specific SMAD involved in the TGF-β1-induced repression of *CYGB*, we used short hairpin (sh)RNAs to stably inactivate *SMAD2* or *SMAD3* in HHSteCs. The shRNA sequences targeted to SMAD2 (shRNA Smad2) and SMAD3 (shRNA Smad3) resulted in 95.6% and 94.2% decreases in SMAD2 and SMAD3 protein levels, respectively (Fig. S7B and C). ShRNA Smad2, but not shRNA GFP or shRNA Smad3, negated the TGF-β1-induced downregulation of *CYGB* expression. Conversely, only shRNA Smad3 reduced the TGF-β1-dependent induction of αSMA, COL1A1, and COL1A2 (Fig. 3E and F). Interestingly, depleting SMAD2 partially attenuated αSMA expression. Next, we confirmed treatment of 3 μM SIS3 completely blocked the TGF-β1-dependent phosphorylation of SMAD3, but not SMAD2 (Fig. S7D). Furthermore, the treatment with SIS3 had no effect on the rhTGF-β1-induced *CYGB* expression, but it suppressed the induction of *αSMA, COL1A1,* and *COL1A2* mRNAs (Fig. S7E). To clarify whether SMAD4 is also part of the complex associated with the reduction of *CYGB* expression, we used an siRNA strategy to knockdown SMAD4 in HHSteCs. SiSmad4 treatment inhibited the TGF-β1-dependent induction of αSMA, COL1A1 and SERPINE1 and the reduction of *CYGB* (Fig. S7F–H). Those results demonstrate that the TGF-β1-SMAD2/SMAD4 pathway is involved in the reduction of *CYGB* expression, and the TGF-β1-SMAD3/SMAD4 pathway is involved in the induction of αSMA, COL1A1, and COL1A2 in HHSteCs.[21]

TGF-β1 mediates the transcriptional repression of *CYGB* via an SP1/3 binding motif in the *CYGB* gene promoter in human HSCs, but not in mouse HSCs

TGF-β1 reduced *CYGB* and increased αSMA and COL1A at the protein and mRNA levels in primary human HSCs (University College London, UK) isolated from the liver tissues of 3 patients (Fig. 4A and B). We also found that 0.4–10 ng/ml rhTGF-β1 failed to repress *Cygb* expression but upregulated *αSma* and *Col1a1* expression in primary cultured mouse HSCs (Fig. 4C and D). To determine the difference in *CYGB* gene regulation by rhTGF-β1 between human and mouse HSCs, we investigated the transcriptional regulatory region of human *CYGB* and mouse *Cygb* and found that an SP1/3 DNA-binding motif was present at the transcription start site (TSS) in human *CYGB* but not in mouse *Cygb* (Fig. 4E and Fig. S8A). SMAD2 has no DNA-binding ability and therefore requires the recruitment of transcriptional co-factors to transmit its regulatory signals.[22] To determine if the TGF-β1/SMAD2-dependent suppression of *CYGB* expression is mediated by SP1/SP3, we used mithramycin A (MTM) to interrupt SP1/SP3 binding to the promoter region. Treatment of HHSteCs with 100 nM MTM completely blocked the TGF-β1-dependent reduction in *CYGB* expression and the upregulation of αSMA, COL1A1, and COL1A2, which is reportedly mediated by the binding of SP1/SP3 protein in fibroblasts[23,24] (Fig. 4F and G). Taken together, the results suggested that SP1 and/or SP3 is involved in the TGF-β1-mediated downregulation of *CYGB* expression in HHSteCs.

The TGF-β1/SMAD2 pathway specifically recruits the M1 repressor isoform of SP3 to the TSS and represses human *CYGB* promoter activity

To test our hypothesis that TGF-β1/SMAD2 targets *CYGB* in human HSCs by recruiting SP1 and/or SP3 to the transcriptional regulatory region, we transfected HHSteCs with a human *CYGB* promoter construct containing the −2133 to +73 nucleotide sequence, which includes the SP1/SP3 binding motif proximal to the TSS in exon 1 of *CYGB*. Treatment of the transfected cells with 2 ng/ml rhTGF-β1 for 48 h resulted in a reduction of human *CYGB* promoter activity, but the reduction was completely abolished by treatment with 100 nM MTM (Fig. 5A). By contrast, rhTGF-β1 did not reduce the promoter activity in HHSteCs transfected with a construct containing the −1726 to +114 nucleotide sequence of the mouse *Cygb* promoter (Fig. 5B). We also transfected primary mouse HSCs with the human *CYGB* or mouse *Cygb* promoter and measured the promoter activity to eliminate potential host effects. Our results indicated that rhTGF-β1 reduced the activity of

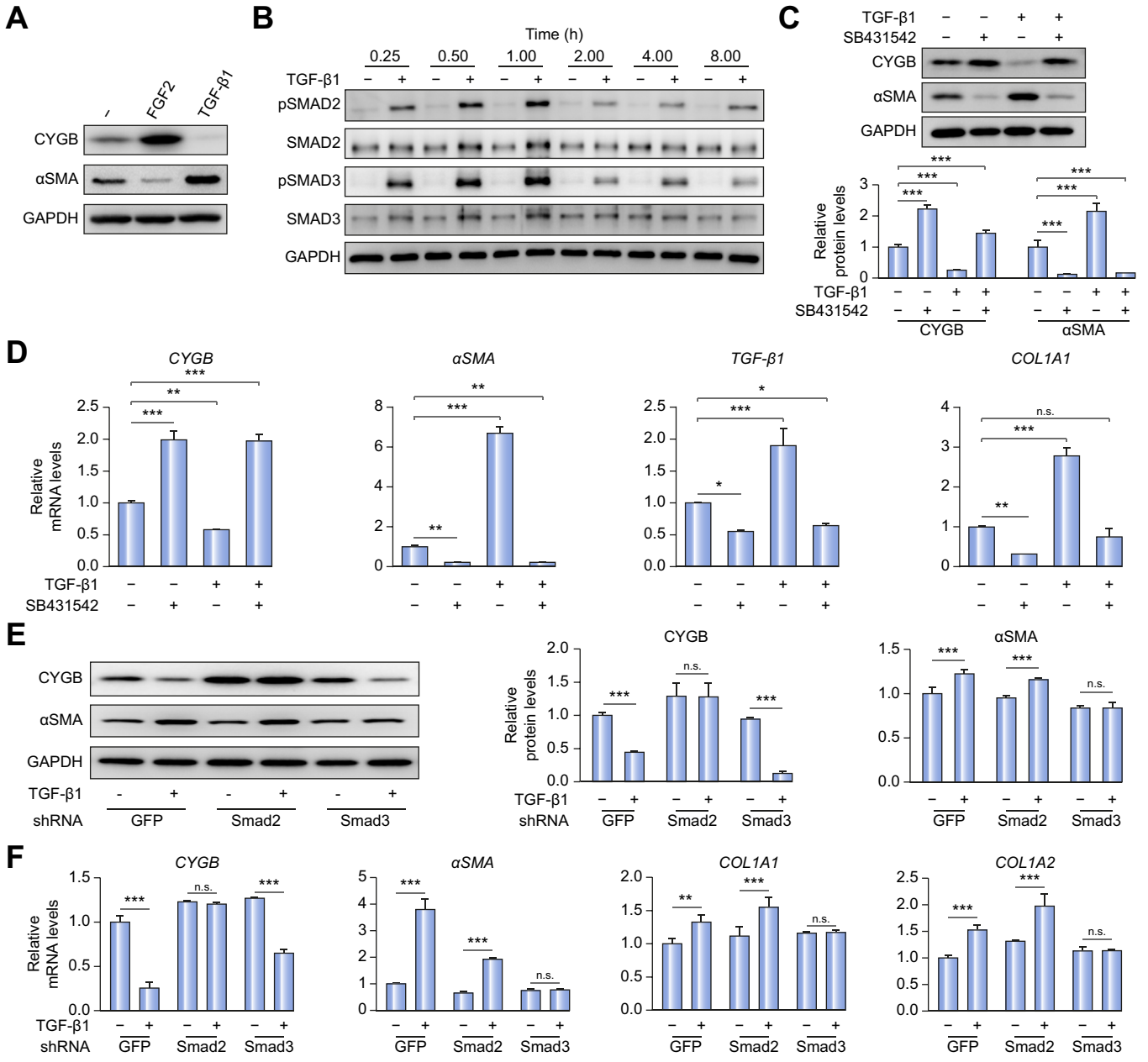

Fig. 3. Effect of TGF-β1 on *CYGB* and αSMA expression. (A) Effect of rhFGF2 or rhTGF-β1 on *CYGB* and αSMA expression in HHSteCs. (B) Expression of total and phosphorylated SMAD2 and SMAD3. (C) Effect of SB431542 on relative *CYGB* and αSMA protein expression. (D) Effect of SB431542 on relative mRNA expression. (E) Relative *CYGB* and αSMA protein expression in HHSteCs transfected with shSmad2 or shSmad3. Bar graphs show relative intensities normalised to GAPDH compared with untreated controls (A, C and E). (F) mRNA levels in HHSteCs transfected with shRNAs. Data expressed as means ± SD, n = 3. n.s.: not significant; $^{*}p$ <0.05, $^{**}p$ <0.01, and $^{***}p$ <0.001 by ANOVA. HHSteCs, human hepatic stellate cells; rh, recombinant human; sh, short hairpin.

the human *CYGB* promoter but not that of the mouse *Cygb* promoter (Fig. 5C).

Next, to examine the binding of SP1 and/or SP3 to the human *CYGB* promoter, we constructed 2 mutated promoters (Mut-1 and Mut-2) with alterations at the SP1/3 DNA-binding motif (5′-GTGGGCGGGCG-3′; labelled No. 4: $^{+}2$–$^{+}13$ nt in Fig. 4E). The inhibitory effect of rhTGF-β1 on the *CYGB* promoter activity was abrogated in both mutants (Fig. 5D). Finally, to determine if SP1 or SP3 was involved in the repression of *CYGB* expression by rhTGF-β1, we used SP1-specific and SP3-specific antibodies to conduct a chromatin immunoprecipitation (ChIP) assay of the *CYGB* promoter region containing the SP1/3 binding motif in HHSteCs (Fig. 5E, left panel). Treatment with 2 ng/ml rhTGF-β1 for 6 h amplified the *CYGB* promoter region that was pulled down by SP3-specific antibody, but not the region pulled down by SP1-specific antibody (Fig. 5E, right panel). The specificity of SP1-specific antibody was confirmed by amplifying the *COL1A2* promoter with the same ChIPped DNA (Fig. S9A). Additionally, we confirmed the TGF-β1-induced recruitment of SMAD2 to the same regulatory region of the *CYGB* promoter for SP3 binding (Fig. 5F). To evaluate the direct interaction between SMAD2 and SP3 in response to rhTGF-β1, we conducted immunoprecipitation

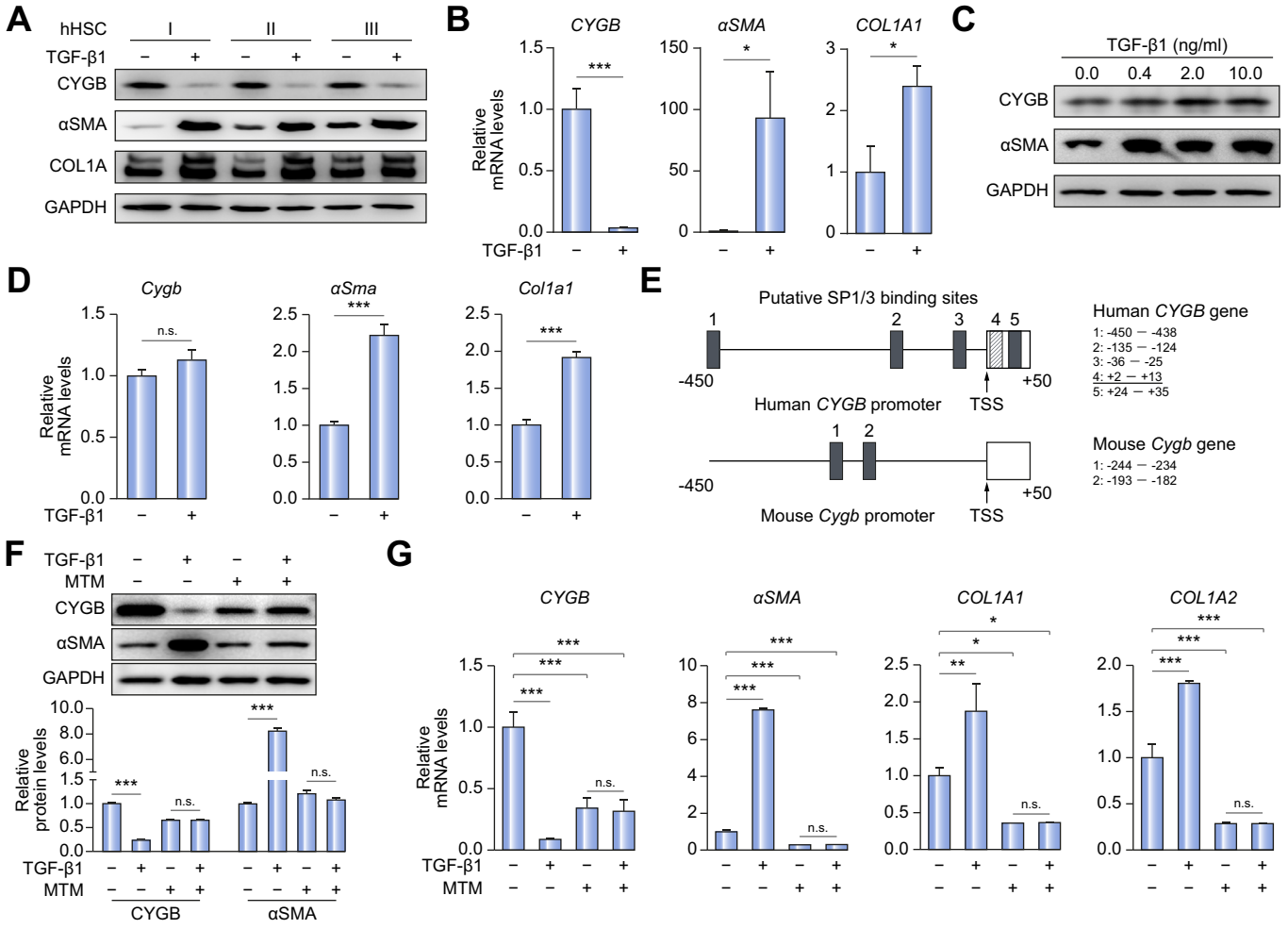

Fig. 4. The effect of TGF-β1 on *CYGB* expression in human and mouse HSCs. (A, B) Effect of TGF-β1 on protein and mRNA levels in human HSCs assayed by western blot (A) and qRT-PCR (B). (C and D) Protein and mRNA levels in mouse HSCs assayed by western blot (C) and qRT-PCR (D). (E) Putative SP1/3 binding motifs (grey bar). Striped grey bar indicates the motif of interest (No. 4). (F) Effect of MTM on relative protein expression in HHSteCs treated with rhTGF-β1 (two-way ANOVA-Dunnett's). (G) Effect of MTM on relative mRNA expression. Data expressed as means ± SD, n = 3. n.s.: not significant; *p <0.05, **p <0.01, and ***p <0.001 two-tailed unpaired t test (B and D) or ANOVA (G). HHSteCs, human hepatic stellate cells; HSCs, hepatic stellate cells; MTM, mithramycin A; qRT-PCR, quantitative reverse transcription PCR; rh, recombinant human; TSS, transcription start site.

with a SMAD2-specific antibody in HHSteCs overexpressing SMAD2. On the basis of previous reports,[25] we deduced that the protein band at 115 kDa corresponded to an activator (full) form of SP3 and that the lower bands were the M1 (70 kDa) and M2 (68 kDa) repressor forms of SP3 in whole-cell protein extracts (Input) (Fig. 5G, left panel). Our results demonstrated that, in parallel to the phosphorylation of SMAD2, which reached the highest level at 1 h after rhTGF-β1 treatment (Fig. S10A), the association of SMAD2 with SP3 isoform M1, but not that with full SP3 or isoform M2, was dramatically increased at 1 h and reduced at 4 h after rhTGF-β1 treatment (Fig. 5G, right panel). Moreover, we confirmed a direct interaction between endogenous SMAD2 and SP3 isoform M1 in TGF-β1-treated HHSteCs (Fig. 5H). To evaluate whether the inhibitory complex between pSMAD2 and SP3 was induced transiently, the nuclear and cytoplasmic proteins isolated from HHSteCs were applied for immunoblot analysis, which confirmed the persistence of SMAD2 phosphorylation and its nuclear localisation up to 24 h after rhTGF-β1 treatment (Fig. S10B and C). Collectively, our results indicate that SMAD2 recruits the M1 repressor isoform of SP3 and suppresses *CYGB* promoter activity following rhTGF-β1 treatment in HHSteCs.

CYGB expression in activated HSCs is negatively correlated with TGF-β1/pSMAD2 signalling in human NASH-related fibrosis

Following our observations in cultured human HSCs, we tested the relationship between *CYGB* expression and the activation of TGF-β1/SMAD2 signalling in human NAFLD/NASH (Table 1). The different stages of fibrosis (F0, F1, and F4) of human NAFLD/NASH were demonstrated by H&E, Sirius Red, and IHC staining of *CYGB*, pSMAD2 and αSMA (Fig. 6A and Table 1). *CYGB*-positive HSCs were abundant in stages F0–2 but scarce in stages F3–4 (p = 0.011; Fig. 6B). Increased Sirius Red staining and IHC staining against pSMAD2 and αSMA was correlated with fibrosis progression (p = 0.0016; Fig. 6A and 6C and Fig. S11A). These results indicate that *CYGB* expression in human NASH is negatively correlated with fibrosis progression.

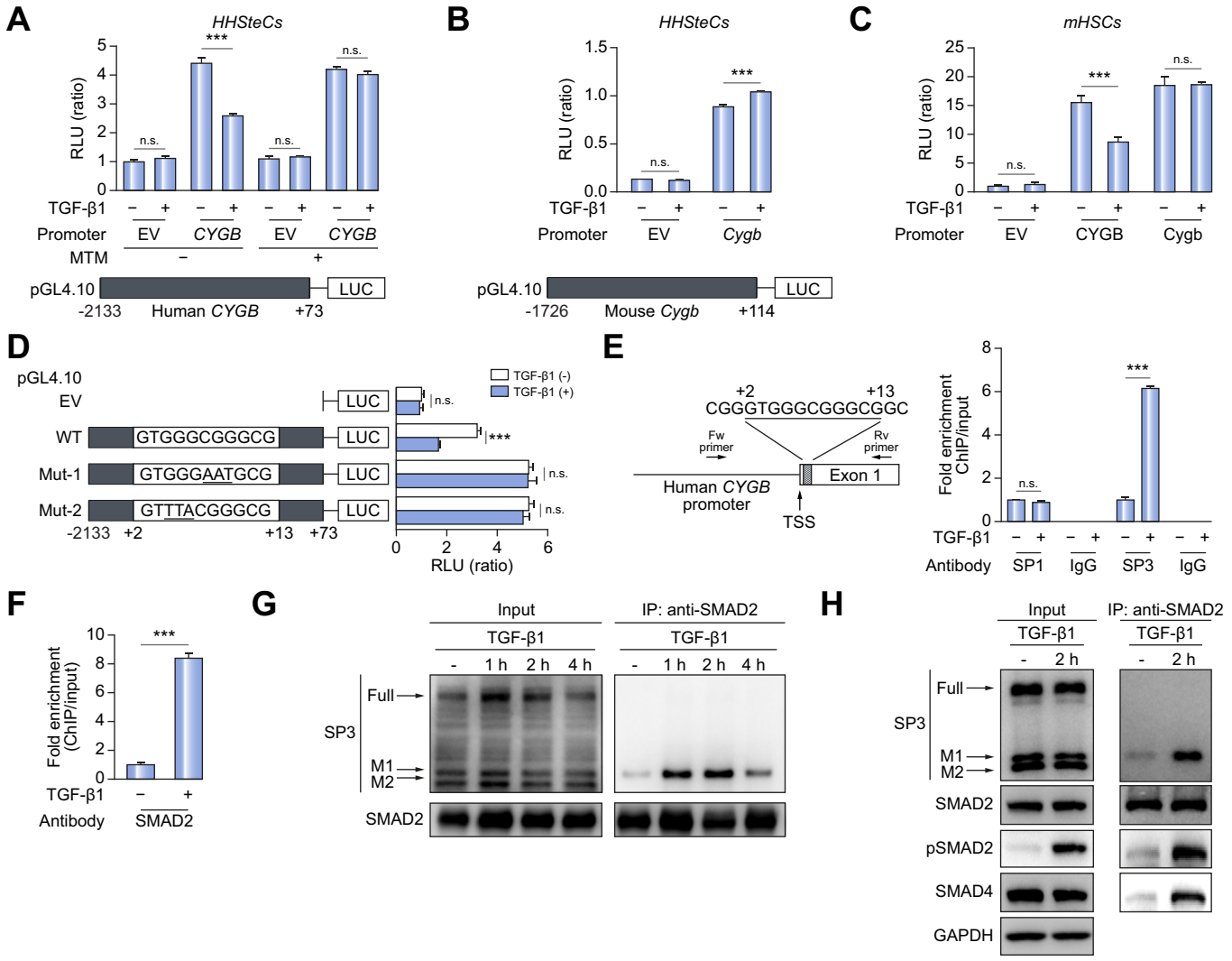

Fig. 5. Regulation of *CYGB* expression by the M1 repressor isoform of SP3 in TGF-β1-treated HHSteCs. (A) *CYGB* promoter activity in (*CYGB*)-transfected HHSteCs. (B) *Cygb* promoter activity in (*Cygb*)-transfected HHSteCs. (C) *CYGB* promoter activity in mouse HSCs. (D) Luciferase reporter fused to wild-type and mutated human *CYGB* promoters (underlined). The pGL4.10-EV vector was used as a control. (E) ChIP using antibodies against SP1 and SP3 and primers targeting the SP1/3-binding motif (grey bar with oblique line). Results analysed by semi-quantitative PCR and presented as fold enrichment relative to total input DNA. IgG was used as a control. (F) ChIP assay of SMAD2 at human *CYGB* promoter was analysed by qRT-PCR. ***p <0.001 by unpaired t test compared with untreated control. (G) IP for the SMAD2-binding protein with TGF-β1 treatment at indicated time points. (H) IP for endogenous SMAD2-binding protein. Data expressed as means ± SD, n = 3. n.s.: not significant; ***p <0.001 by ANOVA (A–D) or two-tailed unpaired t test (E). ChIP, chromatin immunoprecipitation; EV, empty vector; HHSteCs, human hepatic stellate cells; HSCs, hepatic stellate cells; IP, immunoprecipitation; qRT-PCR, quantitative reverse transcription PCR; RLU, relative light unit.

Absence of *CYGB* and pSMAD2 co-expression in activated HSCs along the septum of collagen fibres

In accordance with a previous report on hepatitis C virus-induced liver fibrosis,[26] αSMA and pSMAD2 were co-localised in stromal cells, and the number of double-positive cells was greater in stage F3–4 fibrosis than in stage F0–2 fibrosis (Fig. 7A). IHC staining using NOX4 antibody showed the positivity of NOX4 in both hepatocytes and stromal cells, similar to pSMAD2 IHC staining. Furthermore, αSMA and NOX4 were also co-localised in stromal cells (Fig. S12A and B). Furthermore, we observed *CYGB*-positive cells that were negative for pSMAD2 in liver stroma from patients with F1 fibrosis, whereas we detected no *CYGB*-positive cells proximal to pSMAD2-positive stromal cells in stroma from patients with F4 fibrosis (Fig. 7B). Finally, we observed the co-localisation of 8-OHdG and pSMAD2 in stroma from patients with stage F4 fibrosis (Fig. 7C). Taken together, the results indicate that TGF-β1 signalling is strongly associated with the loss of *CYGB* and oxidative DNA damage in stromal cells from patients with NASH-related advanced fibrosis.

Discussion

Our results revealed that the TGF-β1/SMAD2/SP3-M1 signalling is a key pathway in the downregulation of human *CYGB*, which brings about the accumulation of intracellular •OH and oxidative DNA damage in HSCs from patients with NASH-related advanced fibrosis (Fig. 7D). Hepatic fibrosis can be defined as the persistent production and deposition of ECM by activated HSCs that are stimulated by gaseous, lipid, or peptide mediators secreted by

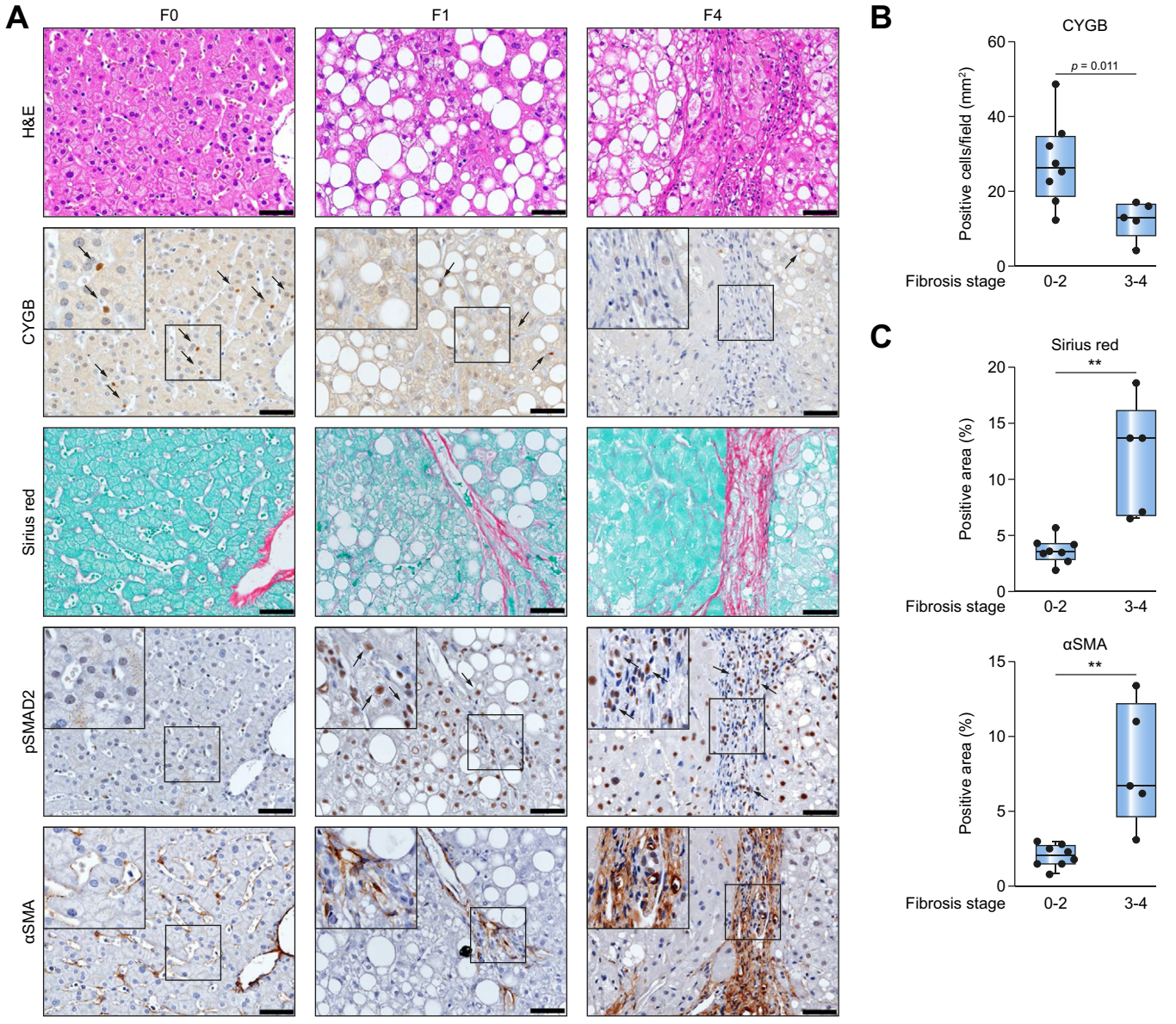

Fig. 6. Expression of *CYGB*, pSMAD2, and αSMA in human NAFLD/NASH biopsy specimens. (A) NAFLD/NASH specimens with the indicated staining. Total n = 13; fibrosis stage F0 (n = 2), stage F1 (n = 4), and stage F4 (n = 2). Arrows, positive cells. Magnified images indicate the same area in each of the stained samples. Bars, 50 μm. (B) Quantification of *CYGB*-positive cells per 1 mm^2 of biopsy specimen. (C) Quantification of Sirius Red-positive and αSMA-positive areas. Data expressed as means ± SD, n = 13 (F0–2, n = 8; F3–4, n = 5). $^{**}p$ <0.01, two-tailed unpaired *t* test (B and C) (see Table 1). NAFLD, non-alcoholic fatty liver disease; NASH, non-alcoholic steatohepatitis.

damaged hepatocytes, mesenchymal cells, and inflammatory cells as a result of cell–cell interactions at the perivascular space.[27] Our results extend the understanding of the mode of TGF-β1 action to encompass the downregulation of *CYGB*, which results in the exacerbation of oxidative DNA damage in human HSCs.

CYGB is highly conserved across species, with 84% and 99% homology between the human and mouse mRNA sequences and protein sequences, respectively (NCBI Blast, https://blast.ncbi.nlm.nih.gov/Blast.cgi). However, contrary to that in human livers with NASH (Fig. 6A and B), hepatic *Cygb* expression markedly increased in mice fed a high-fat diet (Fig. S13A). The difference in *CYGB* regulation between human and mouse livers meant that we could not use *in vivo* mouse models of NASH to investigate the possible link between *Cygb* downregulation by TGF-β1 and the accumulation of •OH in HSCs. Instead, we investigated the mechanistic basis for the difference in transcriptional regulation of *CYGB* in response to TGF-β1 between humans and mice. We identified an SP1/3 binding motif in the TSS of the human *CYGB* promoter that was absent in the mouse *Cygb* promoter. Previous reports showed that SP1/3 independently or cooperatively associates with SMAD2 or SMAD3 to induce *COL1A1* and *COL1A2* transcription and is also required for *αSMA* promoter activation in TGF-β1-induced MFB differentiation.[23,24] Furthermore, TGF-β induces the phosphorylation and nuclear translocation of SMAD2 and SMAD3 primarily in

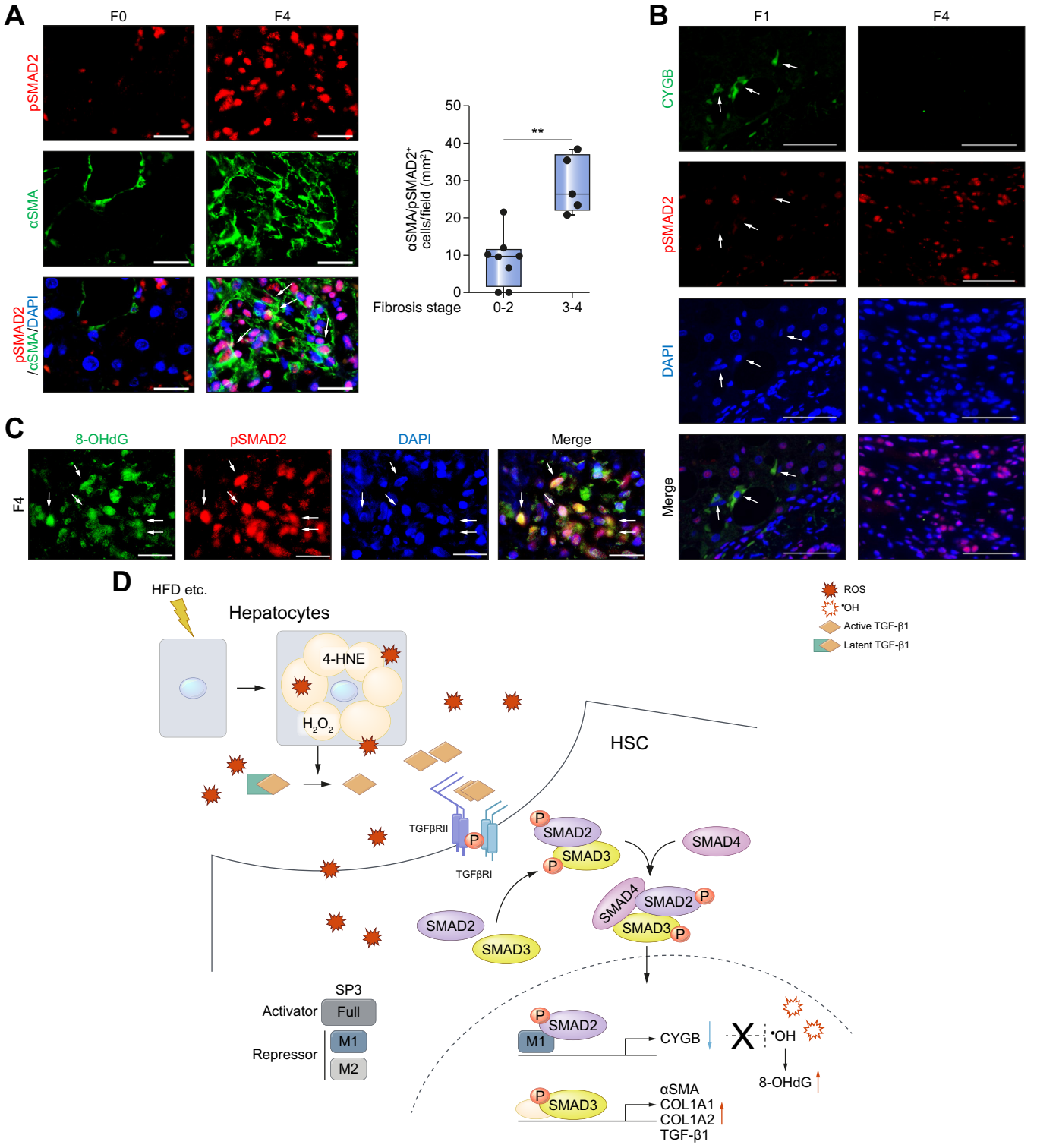

Fig. 7. The association between *CYGB* and pSMAD2 expression in stromal cells from patients with liver fibrosis. (A) Biopsy of fibrosis stage F0 (n = 2) or F4 (n = 2) stained with αSMA (green) or pSMAD2 (red). Arrows, pSMAD2$^+$αSMA$^+$ cells. Bars, 20 μm. Quantification of pSMAD2$^+$αSMA$^+$ cells. Data expressed as means ± SD; total n = 13. $^{**}p$ <0.01; two-tailed unpaired *t* test. (B) Biopsies of F1 fibrosis or F4 fibrosis stained with *CYGB* (green) and pSMAD2 (red). Arrows, CYGB$^+$pSMAD2$^-$ stromal cells. Bars, 50 μm. (C) Immunofluorescence of 8-OHdG (green) and pSMAD2 (red) in F4 fibrosis. Arrows, 8-OHdG$^+$pSMAD2$^+$ stromal cells. DAPI was used for nuclear staining. Bars, 20 μm. (D) *CYGB* involvement in TGF-β1-induced human HSC activation and liver fibrosis. HFD, high-fat diet; HSC, hepatic stellate cell; 8-OHdG, 8-hydroxy-2′-deoxyguanosine.

quiescent and activated HSCs, respectively, and these 2 SMADs have distinct roles in HSC activation.[28] In this study, we found that the TGF-β1-mediated phosphorylation of SMAD2 in human HSCs triggered the recruitment of the M1 repressor isoform of SP3, but not that of other SP3 isoforms. A previous site-directed mutagenesis study revealed that SP1 binding to motifs at nucleotide positions −400, −230, and −210 of human *CYGB* resulted in the upregulation of *CYGB* expression; however, the SP1/3 binding motif at the TSS of interest was not examined in that study.[15] Therefore, the position of the SP3 binding domain (+2) in the promoter region appears to be critical for *CYGB* downregulation. Although the involvement of other transcriptional cofactors in the downregulation of *CYGB* by TGF-β1 should be investigated, our results explain the discrepancy in *CYGB* gene expression between humans and mice.

In accordance with a previous report,[29] we observed the accumulation of 4-HNE in hepatocytes of patients with NASH and advanced fibrosis. HSC activation in the injured liver is primarily initiated by ROS, products of lipid peroxidation, and TGF-β1 released from destroyed/damaged hepatocytes, activated Kupffer cells, and infiltrating inflammatory cells.[30,31] ROS and TGF-β1 are also produced by HSCs in an autocrine manner in response to exogenous ROS and TGF-β1.[32] ROS convert latent TGF-β1 to the active form,[33] and activated TGF-β1 promotes ROS formation by inducing NOX4, thereby creating a vicious cycle.[34] In this study, TGF-β1-induced upregulation of *NOX4* mRNA was suppressed by *CYGB* overexpression, suggesting that *CYGB* may directly regulate NOX4 expression. Furthermore, Fan *et al.* have recently reported that TGF-β1 is secreted as a latent complex and deposited in the ECM of the healthy liver at a high concentration. They found that downregulation of ECM protein 1 in hepatocytes following liver injury strongly increased TGF-β signalling (by spontaneously activating its ECM-deposited latent form) and consequently promoted HSC activation and fibrogenesis.[35]

We investigated the expression levels of *CYGB, GSR, PRDX2* and *TXNRD1* in response to TGF-β1 treatment and found that *CYGB* was the most significantly downregulated by TGF-β1. In many cell types, the transcriptional response to oxidative stress is mediated by a cis-acting element termed the antioxidant response element (ARE); the nuclear factor E2-related factor 2 (Nrf2) has been identified as the most important transcription factor acting on the ARE for many antioxidant genes.[36] Our previous report showed increased Nrf2 expression and reduced TGF-β signalling in transgenic CYGB-overexpressing mouse HSCs.[13] These results suggest the possible coregulation of *CYGB* and other antioxidant genes by their upstream signalling.

The product of DNA oxidation, 8-OHdG, plays a significant role in mutagenesis because of its ability to pair with adenine and cytosine, causing genetic instability.[37] We observed increased 8-OHdG levels not only in hepatocytes[29] but also in MFBs in biopsy specimens from patients with NASH-related advanced fibrosis. TGF-β enhanced the H_2O_2-induced accumulation of •OH in HSCs following the downregulation of *CYGB* expression (Fig. 2B). Furthermore, *CYGB* overexpression abrogated the excessive •OH generation in activated HSCs (Fig. 2C). Interestingly, our observation is supported by a recent study that has demonstrated the accumulation of somatic mutations in the cirrhotic liver, independent of carcinogenesis.[38] The TGF-β1/SMAD2-induced DNA damage in HSCs demonstrated in this study may be associated with early cancer development. Although further investigations of the relationship between oxidative DNA damage and HSC activation during fibrosis development are required, our data indicate that the impairment of antioxidative defence against aberrant •OH accumulation in HSCs is partly due to the downregulation of *CYGB* by TGF-β1.

TGF-β1/SMAD signalling has been shown to be central in the pathogenesis of liver fibrosis; therefore, targeting the TGF-β1/SMAD pathway might be a useful therapeutic strategy for treating liver diseases.[39] At present, there are many strategies to block TGF-β1 signalling. Treatment with neutralising TGF-β1 antibodies or soluble human TGF-β receptor types I and II attenuated liver fibrosis in preclinical models.[39,40] However, therapies targeting the TGF-β1 pathway might also cause adverse outcomes due to pleiotropic effects. We previously reported that FGF2 acts as a *CYGB* inducer in HSCs and promotes the downregulation of αSMA, COL1A1, COL1A2, and TGF-β1. In addition, *in vivo* application of FGF2 attenuated the progression of liver fibrosis in a mouse model of bile-duct ligation.[16] Furthermore, it was reported that overexpression of *Cygb* decreased urinary 8-OHdG excretion and ameliorated kidney fibrosis by suppressing oxidative damage in rats.[41] Thus, accumulating evidence suggests that *CYGB* plays both an antifibrotic and a cytoprotective role, primarily through its antioxidative properties,[10,42] making it a candidate therapeutic molecule for liver disease.

In conclusion, human *CYGB* expression is downregulated by TGF-β1 via a mechanism involving SMAD2 phosphorylation and the M1 repressor isoform of SP3. The downregulation of *CYGB* gives rise to •OH-induced 8-OHdG production in activated human HSCs. Our findings provide new insights into the relationship between *CYGB* expression and the pathophysiology of NASH-related fibrosis in the human liver.

Abbreviations

αSMA, α-smooth muscle actin; ALT, alanine aminotransferase; AST, aspartate aminotransferase; BMI, body mass index; ChIP, chromatin immunoprecipitation; COL1A1, collagen 1α1; COL1A2, collagen 1α2; *CYGB*, cytoglobin; DCFDA, 2′,7′-dichlorofluorescin diacetate; ECM, extracellular matrix; ESR, electron spin resonance; EV, empty vector; FDR, false discovery rate; FGF2, fibroblast growth factor 2; FIB-4, fibrosis-4; GGT, gamma-glutamyltransferase; H_2O_2, hydrogen peroxide; HHSteCs, human hepatic stellate cells; HSCs, hepatic stellate cells; 4-HNE, 4-hydroxy-2′-nonenal; IHC, immunohistochemical; IP, immunoprecipitation; MFBs, myofibroblasts; MTM, mithramycin A; NAFLD, non-alcoholic fatty liver disease; NAS, NAFLD activity score; NASH, non-alcoholic steatohepatitis; NOX4, NADPH oxidase 4; •OH, hydroxyl radical; 8-OHdG, 8-hydroxy-2′-deoxyguanosine; qRT-PCR, quantitative reverse transcription PCR; RFU, relative fluorescence unit; Rh, recombinant human; RLU, relative light unit; ROS, reactive oxygen species; sh, short hairpin; SteCM, stellate cell medium; TGF-β1, transforming growth factor beta 1; TSS, transcription start site.

Financial support

This work was supported by a Grant-in-Aid for Scientific Research (C) from Japan Society for the Promotion of Science (JSPS) KAKENHI JP15K08314 (to MSM) and by a Grant-in-Aid for Scientific Research (B) from JSPS KAKENHI JP16H05290 and a Grant for Research Program on Hepatitis from the Japan Agency for Medical Research and Development (AMED – JP18fk0210004 and JP19fk0210050) (to NK).

Conflicts of interest

All authors declare that they have no financial conflicts of interest to disclose.

Please refer to the accompanying ICMJE disclosure forms for further details.

Authors' contributions

YO, MSM, TM, and NK designed the experiments and interpreted the results. YO, MSM, AD and MK conducted the experiments. KR and LL provided and characterised the primary human HSCs. YO, MSM, TM, KR, LTTT, HI, YM, MK, HF, ME, KI, KY, MP, and NK wrote and revised the manuscript.

Acknowledgements

We would like to express our deepest appreciation to Dr. Lalage M. Wakefield (NCI, NIH), who provided us with the shRNA vectors and comments that greatly improved the manuscript. We also thank Mr. Yuta Noguchi (Doshisha University) for performing the ESR analysis, and the Osaka City University Graduate School of Medicine research support platform for technical assistance.

Supplementary data

Supplementary data to this article can be found online at https://doi.org/10.1016/j.jhep.2020.03.051.

References

Author names in bold designate shared co-first authorship

[1] Fattovich G, Stroffolini T, Zagni I, Donato F. Hepatocellular carcinoma in cirrhosis: incidence and risk factors. Gastroenterology 2004;127:S35–S50.
[2] Asrani SK, Devarbhavi H, Eaton J, Kamath PS. Burden of liver diseases in the world. J Hepatol 2019;70:151–171.
[3] Jun JI, Lau LF. Resolution of organ fibrosis. J Clin Invest 2018;128:97–107.
[4] Weiskirchen R. Hepatoprotective and anti-fibrotic agents: It's time to take the next step. Front Pharmacol 2015;6:303.
[5] Sawai H, Kawada N, Yoshizato K, Nakajima H, Aono S, Shiro Y. Characterization of the heme environmental structure of cytoglobin, a fourth globin in humans. Biochemistry 2003;42:5133–5142.
[6] Liu X, El-Mahdy MA, Boslett J, Varadharaj S, Hemann C, Abdelghany TM, et al. Cytoglobin regulates blood pressure and vascular tone through nitric oxide metabolism in the vascular wall. Nat Commun 2017;8:14807.
[7] Fordel E, Thijs L, Martinet W, Lenjou M, Laufs T, Van Bockstaele D, et al. Neuroglobin and cytoglobin overexpression protects human SH-SY5Y neuroblastoma cells against oxidative stress-induced cell death. Neurosci Lett 2006;410:146–151.
[8] Hodges NJ, Innocent N, Dhanda S, Graham M. Cellular protection from oxidative DNA damage by over-expression of the novel globin cytoglobin in vitro. Mutagenesis 2008;23:293–298.
[9] Li Z, Wei W, Chen B, Cai G, Li X, Wang P, et al. The effect of rhCygb on CCl4-induced hepatic fibrogenesis in rat. Sci Rep 2016;6:23508.
[10] Thuy le TT, Matsumoto Y, Thuy TT, Hai H, Suoh M, Urahara Y, et al. Cytoglobin deficiency promotes liver cancer development from hepatosteatosis through activation of the oxidative stress pathway. Am J Pathol 2015;185:1045–1060.
[11] Thuy le TT, Morita T, Yoshida K, Wakasa K, Iizuka M, Ogawa T, et al. Promotion of liver and lung tumorigenesis in DEN-treated cytoglobin-deficient mice. Am J Pathol 2011;179:1050–1060.
[12] Van Thuy TT, Thuy LT, Yoshizato K, Kawada N. Possible involvement of nitric oxide in enhanced liver injury and fibrogenesis during cholestasis in cytoglobin-deficient mice. Sci Rep 2017;7:41888.
[13] Thi Thanh Hai N, Thuy LTT, Shiota A, Kadono C, Daikoku A, Hoang DV, et al. Selective overexpression of cytoglobin in stellate cells attenuates thioacetamide-induced liver fibrosis in mice. Sci Rep 2018;8:17860.
[14] Fordel E, Geuens E, Dewilde S, De Coen W, Moens L. Hypoxia/ischemia and the regulation of neuroglobin and cytoglobin expression. IUBMB Life 2004;56:681–687.
[15] Guo X, Philipsen S, Tan-Un KC. Characterization of human cytoglobin gene promoter region. Biochim Biophys Acta 2006;1759:208–215.
[16] **Sato-Matsubara M**, Matsubara T, Daikoku A, **Okina Y**, Longato L, Rombouts K, et al. Fibroblast growth factor 2 (FGF2) regulates cytoglobin expression and activation of human hepatic stellate cells via JNK signaling. J Biol Chem 2017;292:18961–18972.
[17] Duvnjak M, Lerotic I, Barsic N, Tomasic V, Virovic Jukic L, Velagic V. Pathogenesis and management issues for non-alcoholic fatty liver disease. World J Gastroenterol 2007;13:4539–4550.
[18] Paradis V, Mathurin P, Kollinger M, Imbert-Bismut F, Charlotte F, Piton A, et al. In situ detection of lipid peroxidation in chronic hepatitis C: correlation with pathological features. J Clin Pathol 1997;50:401–406.
[19] Gandhi CR. Oxidative stress and hepatic stellate cells: a paradoxical relationship. Trends Cell Mol Biol 2012;7:1–10.
[20] Arimoto T, Yoshikawa T, Takano H, Kohno M. Generation of reactive oxygen species and 8-hydroxy-2'-deoxyguanosine formation from diesel exhaust particle components in L1210 cells. Jpn J Pharmacol 1999;80:49–54.
[21] Uemura M, Swenson ES, Gaca MD, Giordano FJ, Reiss M, Wells RG. Smad2 and Smad3 play different roles in rat hepatic stellate cell function and alpha-smooth muscle actin organization. Mol Biol Cell 2005;16:4214–4224.
[22] Zawel L, Dai JL, Buckhaults P, Zhou S, Kinzler KW, Vogelstein B, et al. Human Smad3 and Smad4 are sequence-specific transcription activators. Mol Cell 1998;1:611–617.
[23] Cogan JG, Subramanian SV, Polikandriotis JA, Kelm Jr RJ, Strauch AR. Vascular smooth muscle alpha-actin gene transcription during myofibroblast differentiation requires Sp1/3 protein binding proximal to the MCAT enhancer. J Biol Chem 2002;277:36433–36442.
[24] Zhang W, Ou J, Inagaki Y, Greenwel P, Ramirez F. Synergistic cooperation between Sp1 and Smad3/Smad4 mediates transforming growth factor beta1 stimulation of alpha 2(I)-collagen (COL1A2) transcription. J Biol Chem 2000;275:39237–39245.
[25] Ammanamanchi S, Brattain MG. Sp3 is a transcriptional repressor of transforming growth factor-beta receptors. J Biol Chem 2001;276:3348–3352.
[26] Motoyama H, Komiya T, Thuy le TT, Tamori A, Enomoto M, Morikawa H, et al. Cytoglobin is expressed in hepatic stellate cells, but not in myofibroblasts, in normal and fibrotic human liver. Lab Invest 2014;94:192–207.
[27] Friedman SL. Mechanisms of disease: mechanisms of hepatic fibrosis and therapeutic implications. Nat Clin Pract Gastroenterol Hepatol 2004;1:98–105.
[28] Liu C, Gaca MD, Swenson ES, Vellucci VF, Reiss M, Wells RG. Smads 2 and 3 are differentially activated by transforming growth factor-beta (TGF-beta) in quiescent and activated hepatic stellate cells. Constitutive nuclear localization of smads in activated cells is TGF-beta-independent. J Biol Chem 2003;278:11721–11728.
[29] Seki S, Kitada T, Yamada T, Sakaguchi H, Nakatani K, Wakasa K. In situ detection of lipid peroxidation and oxidative DNA damage in non-alcoholic fatty liver diseases. J Hepatol 2002;37:56–62.
[30] Lee KS, Buck M, Houglum K, Chojkier M. Activation of hepatic stellate cells by TGF alpha and collagen type I is mediated by oxidative stress through c-myb expression. J Clin Invest 1995;96:2461–2468.
[31] Parola M, Pinzani M, Casini A, Albano E, Poli G, Gentilini A, et al. Stimulation of lipid peroxidation or 4-hydroxynonenal treatment increases procollagen alpha 1 (I) gene expression in human liver fat-storing cells. Biochem Biophys Res Commun 1993;194:1044–1050.
[32] De Bleser PJ, Xu G, Rombouts K, Rogiers V, Geerts A. Glutathione levels discriminate between oxidative stress and transforming growth factor-beta signaling in activated rat hepatic stellate cells. J Biol Chem 1999;274:33881–33887.
[33] Wang H, Kochevar IE. Involvement of UVB-induced reactive oxygen species in TGF-beta biosynthesis and activation in keratinocytes. Free Radic Biol Med 2005;38:890–897.
[34] Proell V, Carmona-Cuenca I, Murillo MM, Huber H, Fabregat I, Mikulits W. TGF-beta dependent regulation of oxygen radicals during transdifferentiation of activated hepatic stellate cells to myofibroblastoid cells. Comp Hepatol 2007;6:1.
[35] Fan W, Liu T, Chen W, Hammad S, Longerich T, Hausser I, et al. ECM1 prevents activation of transforming growth factor beta, hepatic stellate cells, and fibrogenesis in mice. Gastroenterology 2019;157:1352–1367.e13.
[36] Nguyen T, Nioi P, Pickett CB. The Nrf2-antioxidant response element signaling pathway and its activation by oxidative stress. J Biol Chem 2009;284:13291–13295.

[37] Maki H, Sekiguchi M. MutT protein specifically hydrolyses a potent mutagenic substrate for DNA synthesis. Nature 1992;355:273–275.
[38] Zhu M, Lu T, Jia Y, Luo X, Gopal P, Li L, et al. Somatic mutations increase hepatic clonal fitness and regeneration in chronic liver disease. Cell 2019;177:608–621.e12.
[39] Xu F, Liu C, Zhou D, Zhang L. TGF-beta/SMAD pathway and its regulation in hepatic fibrosis. J Histochem Cytochem 2016;64:157–167.
[40] Akhurst RJ. Targeting TGF-beta signaling for therapeutic gain. Cold Spring Harbor Perspect Biol 2017;9:a022301.
[41] Mimura I, Nangaku M, Nishi H, Inagi R, Tanaka T, Fujita T. Cytoglobin, a novel globin, plays an antifibrotic role in the kidney. Am J Physiol Renal Physiol 2010;299:F1120–F1133.
[42] Li D, Chen XQ, Li WJ, Yang YH, Wang JZ, Yu AC. Cytoglobin up-regulated by hydrogen peroxide plays a protective role in oxidative stress. Neurochem Res 2007;32:1375–1380.